Energy & Buildings 231 (2021) 110593

Contents lists available at ScienceDirect

Energy & Buildings

journal homepage: www.elsevier.com/locate/enb

Integration development of a Ventilated Active Thermoelectric Envelope (VATE): Constructive optimization and thermal performance

César Martín-Gómez [a], Amaia Zuazua-Ros [a,*], Kattalin Del Valle de Lersundi [a], Bruno Sánchez Saiz-Ezquerra [a], María Ibáñez-Puy [b]

[a] Universidad de Navarra, Department of Construction, Building Services and Structures, Campus Universitario, 31009 Pamplona, Spain
[b] ACR Grupo, Polígono Iruregaña, Aizoain 31195, Spain

ARTICLE INFO

Article history:
Received 24 April 2020
Revised 21 September 2020
Accepted 27 October 2020
Available online 31 October 2020

Keywords:
Architectural integration
Building services
Energy
HVAC
Peltier
Thermoelectricity

ABSTRACT

The use of thermoelectricity in buildings represents a disruptive alternative for indoor thermal needs as it is a technology that allows the elimination of refrigerants. In this line of research, authors of this study have worked on the design and construction of several Ventilated Active Thermoelectric Envelope (VATE) prototypes. A VATE is an industrial-scale modular prototype designed to be installed in the building façade and thought to be an alternative solution for heating and cooling in Net Zero Energy Buildings.

Previous prototype modules have been tested to assess their heat power and performance in heating and cooling mode, which could be considered an initial approach towards the solution of designing VATEs that can be replicated. These works have resulted in an improvement of the COP of the system, the relationship of the Peltier cells and the ventilated façade, as well as with the interaction with photovoltaic systems. However, the problem of the thermal bridge when the VATE was turned off remained.

Taking into consideration the lessons learned from previous construction solutions, the system has been redesigned, prioritizing in this case the reduction (not elimination) of the VATE thermal bridge. This article describes and justifies the solutions developed, presents the results achieved for heating and cooling, and raises points about what could evolve from this issue.

1. Introduction

Thermoelectric phenomena has been widely discussed [1]. Generally speaking, this effect is created when an electrical current passes through a semiconductor group of unions. Depending on the direction of the current, one side of the cell will absorb heat and release it into the other, and if the current direction changes, the effect is reversed. Several studies have been developed to understand the process of heat transference. They analyze in detail different materials, manufacturing techniques, costs, geometrical effects and consumption. In recent years the number of studies which focus on the practical applications of thermoelectricity has increased significantly. One of these applications is the use of thermoelectricity as a heating and cooling system for buildings [2].

Despite the use of thermoelectricity as an available solution on the market being in the long term future, [3], the quantity of research which has been carried out related to its use as a heating/-cooling system has increased in recent times [4]. Most of this research proposes a Thermoelectric Cooling and Heating Unit (TCHU) which is not integrated into the building façade, indicating that it primarily focuses on the development of the system as a 'tool, providing data related to the COP of the system [5] and its comparison to other conventional heating and cooling systems [6]. Some of these studies explore the possibility of integrating the TCHU into different construction elements, such as window, façade or roof/dwelling, as studied in the review recently published [4].

Nevertheless, none of these publications and projects attempt to analyze the factors that affect the integration of the Peltier cells from the point of view of construction. Moreover, concepts such as heat loss through construction elements, durability, acoustic performance, aesthetics or fire behavior are barely mentioned. These could be considered essential parameters for the system.

Authors of this study have been working on the design of a Thermoelectric Cooling and Heating Unit (TCHU) since 2009, which was later defined as Ventilated Active Thermoelectric Envelope (VATE). All of these previous projects were aimed at finding an innovative, modular and autonomous heating and cooling system for buildings embedded in the building envelope. The methodology

* Corresponding author.
E-mail address: azuazua@unav.es (A. Zuazua-Ros).

https://doi.org/10.1016/j.enbuild.2020.110593
0378-7788/

used throughout the different studies was based on the construction of real scale prototypes monitored under real conditions. The different goals achieved over these years can be summarized in the following milestones:

- First real-scale VATE prototype (2009–2011). This first unit led to a new patent. It demonstrated that it is possible to cool or heat a space with thermoelectric devices. The importance of improving the energy performance of the unit as a façade element was also discovered [7,8,9] (Fig. 1.a).
- Second real-scale VATE prototype (2014–2017). On this occasion, the integration of the system into a ventilated façade was the principal challenge [10]. As a consequence of the improvements made, the results highlighted the thermal bridge generated by its own thermoelectric devices [11–13] (Fig. 1.b).
- Third real-scale VATE prototype (2016–2018). The objective of this prototype was to create a design which was modular (easy to assemble, P&P solution) and autonomous (PV panels) VATE. It represented an important step forward, especially in those aspects related to the thermoelectric control system. However, the design failed in several areas related to energy performance as a façade: there was a lack of airtightness as well as heat loss due to the lack of insulation and the thermal bridges generated by the Peltier cells [14] (Fig. 1.c). These two factors, together with an optimization of the number of cables and final laying, are perhaps the main advances of the prototype developed for this study compared to that previously mentioned in [14]. Other minor but notable improvements will also be detailed.

Thermoelectricity is based on the use of Peltier cells, which currently have relatively small dimensions and low heat transfer capabilities. This means that in order to heat or cool a space it is necessary to use a considerable number of them. As has been demonstrated beforehand, this poses a problem for certain uses, but it also offers the advantage of modulation, so if the operation of a part is known, the results can be extrapolated to the entire system. As a consequence, the results and conclusions of these three real-scale experiences have been complemented with two small scale prototypes:

- Adiabatic box. Before the design of the third prototype, a small-sized adiabatic box was built, in which different combinations of diffusers, fans, fasteners and electrical connections were tested. After several tryouts, the solution of the box module gave rise to the final decision for the complete prototype [15].
- aBox. Taking into account all of the previous experiences, another small sized adiabatic box was designed which helped test different options and come up with a final design that allowed the maximum avoidance of the thermal bridge generated by the Peltier cells.[16] (Fig. 2).

Fig. 2. aBox prototype. The development of this was essential for the design of the aluminum elements created to reduce the thermal bridge that guarantees the pressure between the heat sink and the TEM.

In this article, the latest optimized VATE design is presented, the drawbacks arising from the Peltier cell thermal bridge are faced and a new constructive design is proposed, with the following objectives:

- Describe in detail the optimization of the integration of a thermoelectric module in the façade, improving the constructive system definition, the airtightness and thermal behavior.
- Optimize the thermoelectric system, components space, the electric board, the connections and control system.
- Analyze the operating behavior data for cooling and heating.

2. About the constructive definition

This section describes the constructive parameters of both the room where the prototype is installed and the prototype itself. The space to be conditioned is the same as the room where the previous prototype was installed (Fig. 1.c). However, several improvements were made, given the age and conditions of the existing building.

2.1. Test room construction improvements

Fig. 3 corresponds to the test room plan, which is an 11 m^2 office space with a window oriented to the northeast. With the aim of carrying out the tests in optimal environmental conditions the test room was renovated, improving thermal and air tightness conditions.

The renovation proposed aimed to create a low energy consumption space. This is justified because one of the lessons learned from previous prototypes is that the inherent behavior of

Fig. 1. Evolution of VATE prototypes (2009–2018).

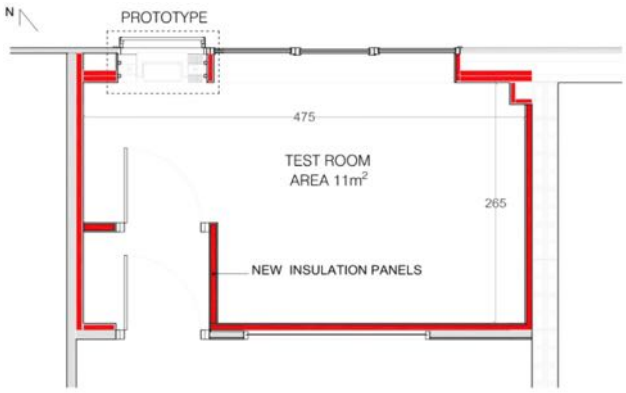

Fig. 3. Plan of the renovated test room (dimensions in centimeters). The red color refers to insulation reinforcements. A previous small hall was built to ensure additional isolation of the room from the adjacent space. (For interpretation of the references to color in this figure legend, the reader is referred to the web version of this article.)

thermoelectric components does not make for good U-values, and physical construction of these spaces should be as efficient as possible. Due to this, the following modifications were undertaken:

- Insulation of the room in all the enclosures. For the floor, two boards of 50 mm of rigid polyisocyanurate foam were installed, for the vertical surfaces 50 mm of mineral wool and a mineral wool panel of 200 mm installed in the suspended ceiling. The modular suspended ceiling was replaced by continuous drywall panels.
- Replacement of the window. A triple pane window filled with argon gas was installed to replace an old single panel window. The dimensions of the opening were maintained.

Table 1
U-values of the construction elements of the room.

Building elements	U-value[W/m^{2}K]	U-value from CTE [W/m^{2}K]
Façade	0.34	0.66
Indoor walls	0.53	0.85
Window	1.11	2.50
Roof (ceiling)	0.17	0.38
Floor	0.16	0.49

- Sealing of the façade joints with adhesive sealing tapes to ensure airtightness.

A heat recovery system (maximum airflow of 210 m^3/h) was also installed, principally for the winter season, in order to reduce the heating demand. Therefore it was not used in this experimental set. Furthermore, as in previous prototypes, the internal loads of the room were not taken into account for the research.

The final theoretical U-values of the room envelope achieved after the renovation are gathered in Table 1. The right hand column of the table shows the values that the Spanish Building Technical Code (CTE) requires for this type of building in the same climate zone. As shown, the values obtained after the renovation are far from the regulated limit.

2.2. Prototype construction

The prototype breaks down into three elements: left module, right module and electrical panel. The left and right modules are fitted with 8 Peltier cells each, 2 axial fans and 2 heat sinks. The module in the middle is the electrical panel board. For the entire assembly of elements, 1–2 cm thick DM panels were used, where the pieces could be screwed. In the spaces between the different DM panels, extruded polystyrene (XPS) rigid panels were placed to ensure insulation. Likewise, a substructure of aluminum profiles served as a support for the entire prototype in the facade (Fig. 4).

In the inner part, the prototype lies flush with the inner face of the façade, however, in the outer face, the prototype is tucked into the air chamber of the ventilated façade, ending with aluminum carpentry of outward-facing fixed slats.

The electrical panel is placed between the left and right module, which contains all of the control and data collection devices. The frame of the electrical panel is screwed to the DM panel on the back. As indicated in the horizontal constructive section (Fig. 4), 50 mm thick XPS panels surround the electrical panel, which assure the isolation of the module from external conditions.

2.2.1. Construction of the modules

To minimize the thermal bridge that was generated in the iACTIV 1.0 prototype (Fig. 1.c), a more compact module was designed and the generation of a hole in the interior was avoided (Fig. 5). There are two main constructive differences with iACTIV 1.0:

1. The interior gap between heatsinks was filled with XPS rigid panels reducing the thermal bridge.

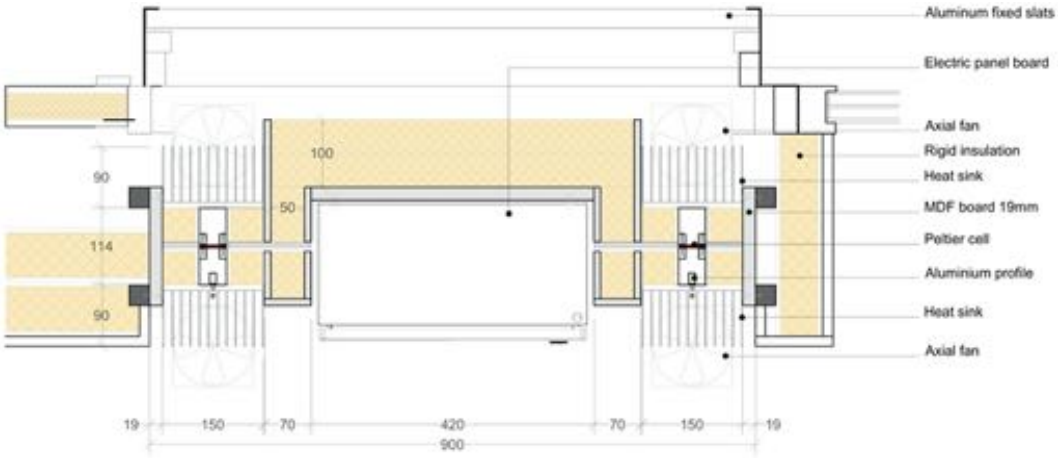

Fig. 4. Horizontal construction section. The yellow color corresponds with the insulation. The position of the electric board between the two modules allows a simpler disposition of the wires. (For interpretation of the references to color in this figure legend, the reader is referred to the web version of this article.)

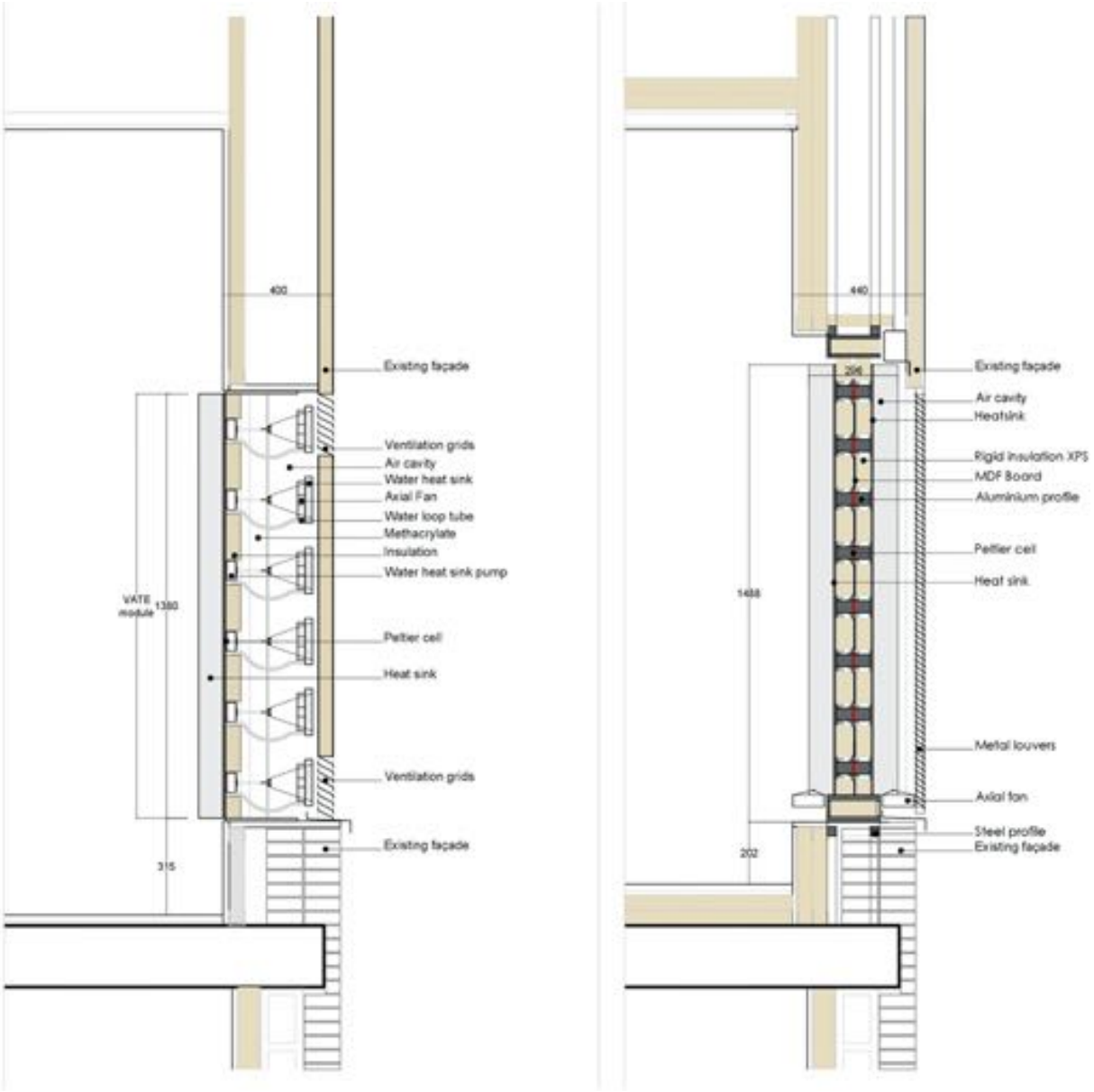

Fig. 5. Evolution of the construction section of the third real-scale VATE prototype (left, 2016) and the one explained in this article (right, 2019). The yellow color refers to insulation, verifying how both the internal space and the active facade itself have been improved. (For interpretation of the references to color in this figure legend, the reader is referred to the web version of this article.)

2. Peltier cells were embedded inside two elongated solid pieces of aluminum (6082 alloy). These pieces were designed specifically for this prototype and allow the regulation of the pressure on the Peltier cells and a space to accommodate the temperature sensors on both sides of them. Each module is composed of 8 Peltier cells.

With regard to heatsinks, each module is designed to be built from inside the room, which is why the aluminum solid profiles of the outer module are welded to the outer heatsink. However, in the inner heatsink the aluminum profiles are screwed. This permits building on the facade without the need to access it from the outside. This is an important design decision with regards to looking to the future of the implementation of VATE in real buildings.

The fact that the interior aluminum solid profiles are screwed allows access to the Peltier cells and the sensors by exclusively dismantling the internal heatsink. The heatsinks are 6060 aluminum alloy.

In order to record and control the exact temperature of the Peltier cell faces, an NTC sensor was placed on each of the faces. To ensure the correct contact of the probes with the surface of the face, 0.5 mm grooves were designed on the inner faces of the solid aluminum solid profiles. This guaranteed the position and contact of the NTC probe with the Peltier cell during the tests. Likewise, the aluminum parts have four inner tabs so that the two pieces of solid aluminum can be screwed together, in this way ensuring the correct pressure of the aluminum parts with the Peltier cell. (Fig. 6). In the opinion of the authors, this design represents an important advance in quality which will be used in further prototypes.

The aluminum elements are 4×4 cm with 5 cm length. The addition of this component hinders the heat transfer between the TEM and the vertical heat sink. A brief independent experimental

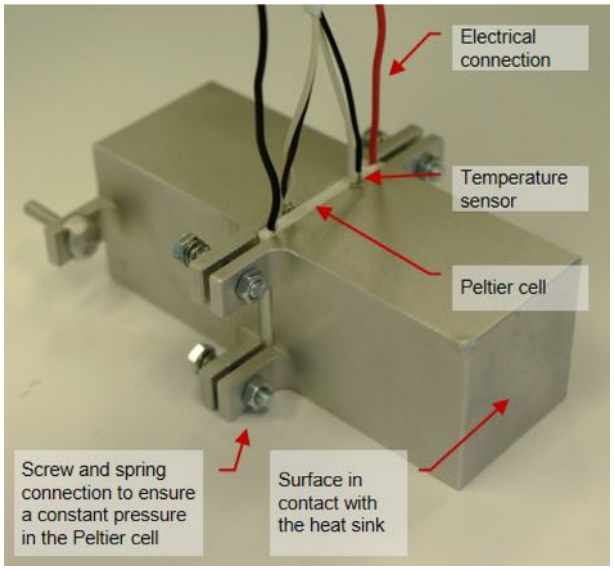

Fig. 6. Image of the aluminum elements designed to reduce the thermal bridge that guarantees the pressure between the heat sink and the TEM.

analysis of the element was carried out in order to assess the performance and the time needed to achieve the thermal inertia between the inner and outer faces of the aluminum element at different voltages. Four temperature sensors were used, two in the hot and cold faces of the TEM and the other two in the aluminum surfaces in contact with the heat sinks. All the tests were carried out in laboratory conditions at an ambient temperature of between 22.3 °C and 24.0 °C.

Table 2 shows the temperature differences between the TEM faces and the two aluminum outer surfaces for different voltages after 30 min tests. The cold side of the Peltier cell reaches similar temperatures at almost every voltage. This leads to a low difference of $T_{heatsink}$ - T_c, meaning that at such ambient temperatures and working voltage, both the aluminum element and the cell function at close temperatures. As a consequence, the aluminum element does not offer significant resistance on this side. The higher the voltage, the lower the temperature difference on the cold side, as opposed to the hot one. At a higher voltage, the temperature difference of the cold side is more stable. It should be noted that at a temperature difference that low, a more accurate test should be done in order to study the temperature difference variations in the scenarios of 6 V and 8 V, as shown in the graph on the left in Fig. 7. However, on the hot side, the higher the voltage, the higher was the difference in temperature. This is illustrated in the graph on the right in Fig. 7. After 5 min tests, in most cases the temperature difference stabilized.

Table 2
Temperature differences between the TEM's hot and cold faces and their corresponding part of the opposite end of the aluminum element.

Voltage [V]			Temperature differences	
	T_c [°C]	T_h [°C]	$T_{heatsink,c}$ - T_c	T_h - $T_{heatsink,h}$
6 V	7.19	42.01	1.56	8.22
8 V	7.22	51.55	1.47	12.83
10 V	5.20	57.87	1.04	17.98
12 V	7.75	68.18	0.87	23.58

Therefore the inclusion of the aluminum element can cause a reduction in temperatures of up to 23 °C on the hot side of the system, reducing the heat sink temperature and making heat dissipation more difficult, since the thermal leap between the sink and the outdoor ambient temperature is lower.

3. Optimizing the wiring data and electrical system integration design

The electric connections, the arrangement of the Peltier cells and the monitoring equipment were optimized to achieve a more effective performance and integration. This is consequently the first step towards the complete constructive integration of the system in a façade, including the electric board and control system. It must be taken into account that the thermoelectric system itself and the installed control system for monitoring require a considerable volume of wiring, electrical protection, control cards and data loggers. The layout of all of these components must be designed and optimized because when the amount of cable and wiring is high, the risk of poor thermal behavior as a façade is also higher. In this fourth prototype, there is a reduction in volume by half compared to the third prototype, bringing it closer to the needs of a more realistic system.

3.1. Arrangement of the TEMs

Due to the increase in insulation and the new window installation, the energy demand of the room is reduced. In this way the number of TEMs installed in the prototype changes from 24 units

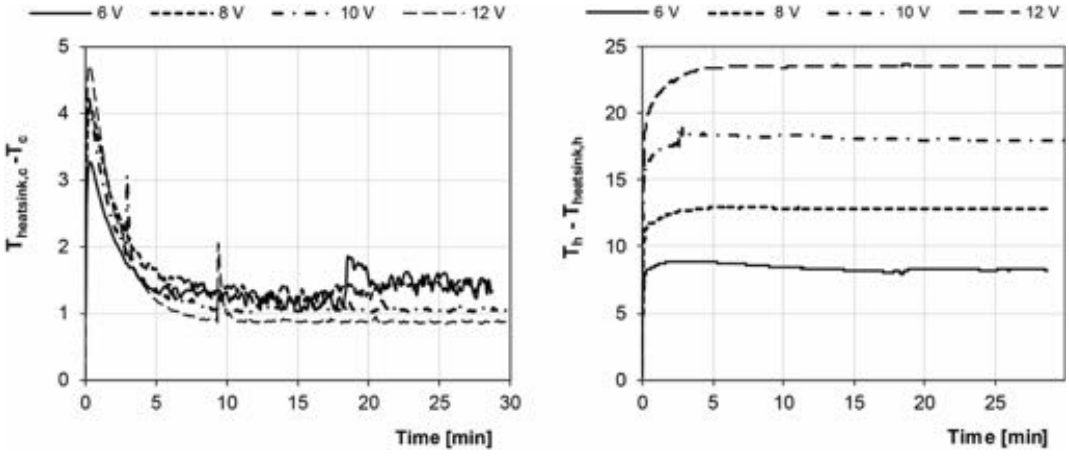

Fig. 7. Temperature difference of the cold side (left) and hot side (right) between the face of the Peltier cell and the respective end of the aluminum element at different voltages after a 30 min test.

(in the previous prototype) to 16. Regarding the installed power capacity, the previous TEMs corresponded to 1200 W and the new arrangement was 848 W. The TEMs used in this prototype are CP60440 model [17] (Table 3).

The 16 TEMs were divided into two vertical modules. The arrangement of each set of 8 cells was made by connecting pairs of cells in a series and then grouping them in parallel to create two channels of 4 cells, as represented in Fig. 8.

3.2. Control system

Fig. 8 illustrates the diagram of the configuration of the electrical connections and control system. The temperature of the faces of the TEMs, room and outdoor air cavity temperatures and the electrical consumption is monitored and measured. Each cell has two NTC sensors (JT Thermistor 103 JT-025) measuring the temperature of each face.

The control of the intensity and current for the TEMs is done with two control cards (TEC 1122-SV model [18]). Each card has two channels and collects the temperature data from two Peltier cells. Each card controls a vertical module from the condition of two TEM. The temperatures of the remaining TEM are monitored with two data logger PicoLog 1012 models. There is a third control card (TEC 1090 model) which gathers the indoor ambient temperature and enables the relation between this room temperature and the performance of the TEMs. The room temperature is measured by PT-100 sensors (EGT354F102 model).

The indoor and outdoor fans are also connected to the control cards, which supply the necessary power at 24 V and control their operation as well as through PWM control function. The outdoor fans have an ingress protection of IP68. Even though they are protected by louvers in the facade, they are exposed to the external climatic conditions.

Table 3
Characteristics of the Thermoelectric Module and fans used.

	Specification	Value
Thermoelectric module	Hot side temperature	298 K
	Q_{max}	53 W
	ΔT_{max}	68 K
	I_{max}	6.0 A
	V_{max}	15.4 V
	Resistance	2.17 Ω
Outdoor fan	Dimensions	120 × 120 × 38 mm
	Airflow (max)	182 CFM
	Rated voltage	24 V
	Rated current	0.8 A
	Ingress protection	IP68
Indoor fan	Dimensions	120 × 120 × 25 mm
	Airflow (max)	146 CFM
	Rated voltage	24 V
	Rated current	0.47 A

3.3. Wiring

The connections of the elements have a relevant role with relation to the physical integration of the module in the façade. In the previous experience, the electric board that powered and controlled the Peltier cells was located inside the testing room but independent from the thermoelectric module. This location complicated the supply connections, where the wiring integration was not achieved.

The same aspects were monitored in both projects, the difference being the location of the electrical panel. In the second project it is in the middle of the prototype which resulted in a shortening of the wire.

In this case, the electric board is located between the two vertical modules (see Fig. 9) which simplifies the supply connections. The 24 V power supplies and the energy meter are situated in an independent electric board outside the room.

4. Performance of the system

Cooling and heating mode tests were carried out. The prototype was tested under different voltage conditions for two hours each time (6, 8, 10 and 12 V). As demonstrated previously, the performance of the prototype was better in all cases with the fans working [14], as both indoor and outdoor fans were functioning in the tests. To calculate the heat absorbed and released by the TEMs, the following equations (1–2) were used [19].

$$Q_c = S_m\hat{A}\cdot I\hat{A}\cdot T_c - \frac{1}{2}\hat{A}\cdot R_m\hat{A}\cdot I^2 - K_m\cdot(T_h - T_c) \quad (1)$$

$$Q_h = S_m\hat{A}\cdot I\hat{A}\cdot T_h + \frac{1}{2}\hat{A}\cdot R_m\hat{A}\cdot I^2 - K_m\cdot(T_h - T_c) \quad (2)$$

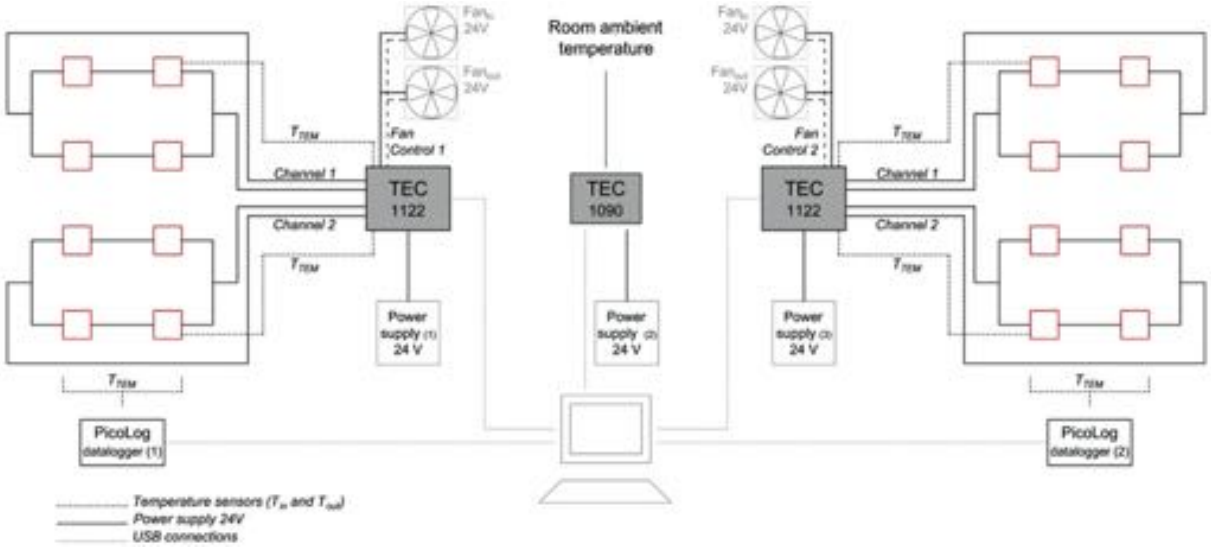

Fig. 8. Arrangement of the electrical and control system. Note that each group of four Peltier cells are commanded by a common sensor.

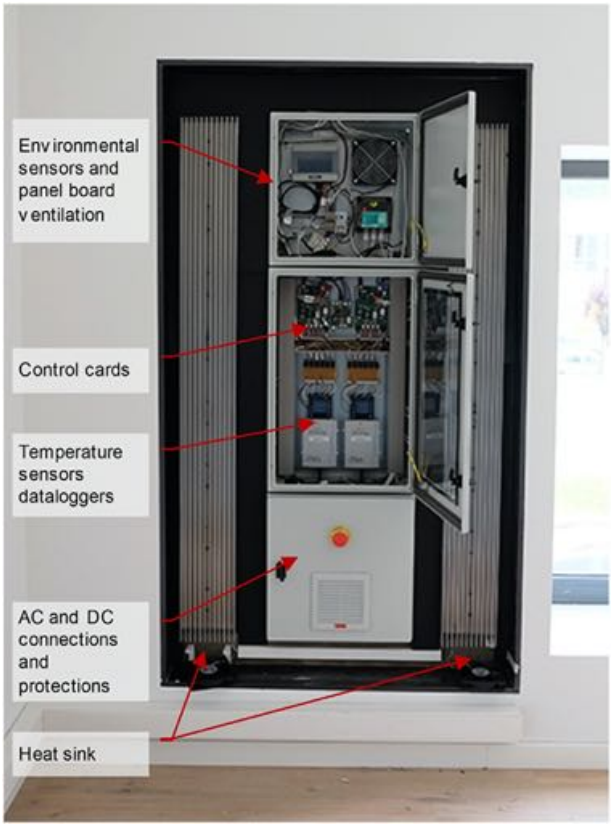

Fig. 9. Front view of the prototype installed in the room. The electric panel is divided into three boards. The bottom one includes the connections, protections and emergency button. The main control and monitoring elements are located in the middle panel. At the top there are external sensor data loggers and the ventilation fan for the board.

In these equations, the Seebeck coefficient (S_m), electrical resistance (R_m) and thermal conductance (K_m) are the terms given by the characteristics of the TEM used, together with the figure of Merit, which are calculated using equations (3–6):

$$S_m = \frac{V_{max}}{T_{h0}} \tag{3}$$

$$R_m = \frac{(T_{h0} - \Delta T_{max})\ \Delta\ V_{max}}{T_{h0}\ \ I_{max}} \tag{4}$$

$$K_m = \frac{(T_{h0} - \Delta T_{max})\ \cdot\ V_{max}\ \cdot\ I_{max}}{2\ \cdot\ T_{h0}\cdot\ I_{max}} K_m = \frac{(T_{h0} - \Delta T_{max})\ \cdot\ V_{max}\ \cdot\ I_{max}}{2\ \cdot\ T_{h0}\cdot\ \Delta T_{max}} \tag{5}$$

$$Z = \frac{S_m^2}{R_m \cdot K_m} \tag{6}$$

After the calculation of the electrical power needed by the TEMs (Q_e), which is the product between the current and voltage, the COP can be measured with an equation (7):

$$COP = \frac{Q}{Qe} \tag{7}$$

In the cases where the consumption of the fans was also considered in the total consumption, the term of the performance is COP_f.

4.1. Analysis of temperatures

The cooling mode tests were carried out during July 2019, when the outdoor temperatures varied between 26 °C and 33 °C. The tests in heating mode were undertaken between December 2019 and January 2020, when the outdoor temperature varied between 6 °C and 13 °C.

The temperatures in Fig. 10 correspond to the difference in average temperature value between the faces of the Peltier cell for each input voltage scenario. In general, after a 45 min test the temperatures stabilized and maintained constant. In either mode, the higher the voltage, the higher the temperature difference, which would convert into not only a higher cooling or heating capacity, but also a higher consumption. The temperature difference which can be reached in heating mode is higher than that of in cooling mode due to the affection of Joule effect in cooling.

Regarding the temperature achieved by the inner faces of the TEMs, as shown in Fig. 11, the cells need about 30 min to stabilize the face temperatures. In cooling mode, after this time, in some voltages the temperature increases slightly, which could be caused by the high temperature of the room. The case of 12 V is the most representative. The authors consider that this is due to room temperature, which is always higher due to high outdoor ambient temperatures and the high insulation of the room. Consequently, the system depends first on the thermal inertial of the heat sink, and secondly, on the heat transfer between the room ambient temperature and the heat sink.

In heating mode, the temperatures which can be achieved depending on the voltage are in a wider range than those achieved

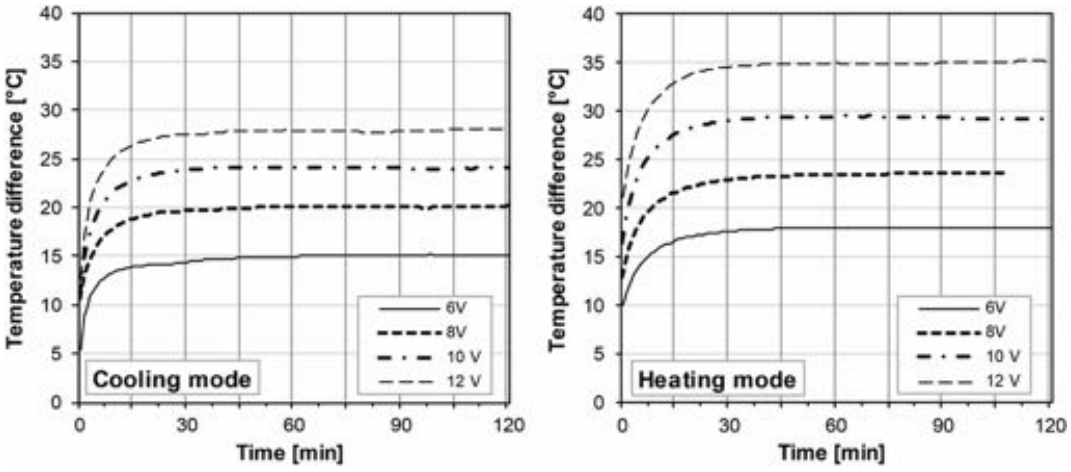

Fig. 10. Temperature difference between the faces of the TEM for a two hour test for each input voltage.

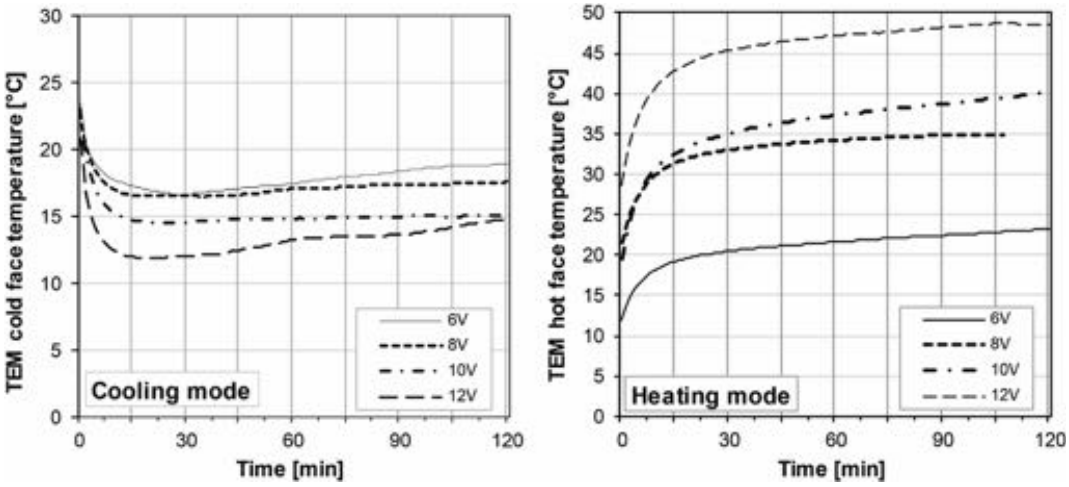

Fig. 11. Temperatures of the inner faces of the TEM during the tests at different voltages.

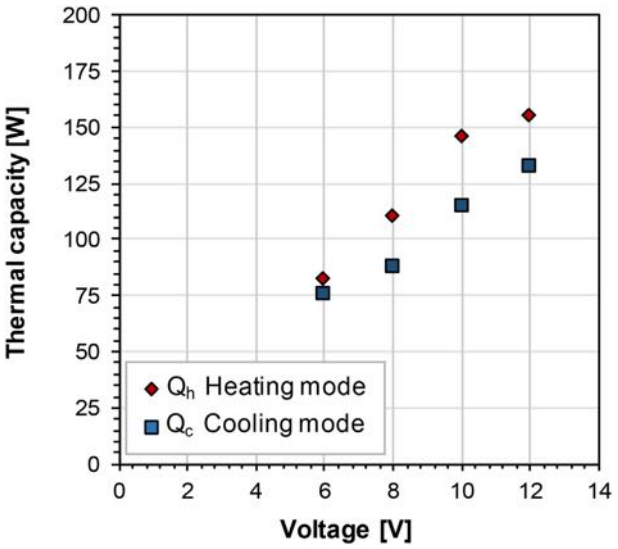

Fig. 12. Cooling and heating capacity of the prototype regarding the input voltage.

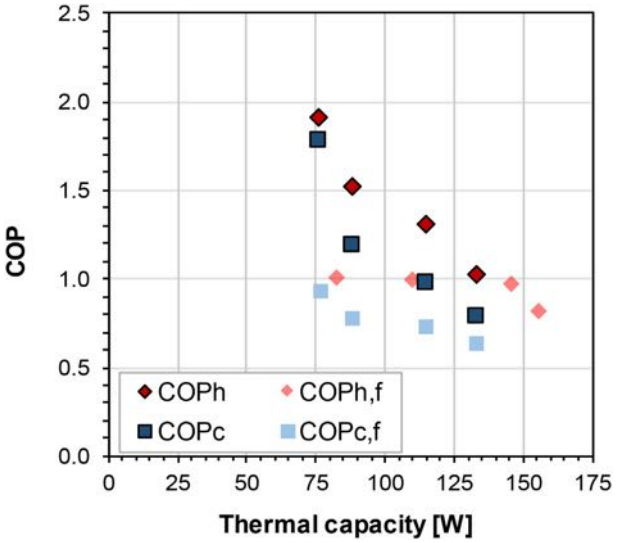

Fig. 13. COP of the system regarding the cooling capacity.

in cooling mode. In 12 V scenario, the inner face temperature is double the one at 6 V.

4.2. Analysis of the performance

Both the cooling and heating power of the complete prototype are calculated for each mode with Eq. (1) and (2). The temperature difference between the faces is a negative value regarding the cooling capacity calculation, as the higher the temperature difference, the higher the cooling or heating power. However, this increase is due to the rise in voltage and consequent rise in the current, which results in a greater amount of net power related to temperature difference. As illustrated in Fig. 12, the net cooling capacity varies between 53 and 133 W depending on the input voltage. This graph represents the cooling capacity at the end of each test. In heating mode, the heating capacity as expected, is higher, varying between 82 and 155 W.

Concerning the relation between thermal capacity and the COP, Fig. 13 indicates that the COP decreases considerably as the thermal capacity increases, due to the higher electricity consumption of the system at a higher voltage. The values of the COP in cooling mode vary between 0.79 and 2.70, and between 1.02 and 1.91 in heating mode.

When comparing the COP of the system in relation to fan consumption, as expected, the COP decreases. In this case, the fans used operated at 24 V in comparison to the fans used in the previous prototype, which worked at 12 V. In this way the minimal difference between the two COP in the previous heating experiments, increases in this example, the case being extreme at lower voltage, where the COP_f is almost two times lower than the performance without the fans. The consumption of the fans in this instance could therefore be considered a decisive value for the final performance.

The consumption of the auxiliary equipment was a subject of discussion. It has been demonstrated that for thermoelectric generators, it is necessary to bear in mind that consumption can affect the net generation considerably [20]. The same occurred in the VATE prototype assessed in this case (Fig. 13); the consumption of the fans affected the COP.

Tables 4 and Table 5 gather the values of the main parameters after 2 h tests for cooling and heating modes respectively. The drop in the COP when considering fan consumption can be clearly seen in the last two columns on the right. In cooling mode, the $COP_{c,f}$ does not reach the value of 1 in any of the scenarios tested. That said, if fans are not taken into consideration, the value is only

Table 4
Summary of the values of main parameters at the end of each cooling mode test.

	T_c	T_h	ΔT	Q_c	COP_c	$COP_{c,f}$
6 V	18.94	34.03	15.10	76.42	1.78	0.94
8 V	17.60	37.83	20.23	88.39	1.19	0.78
10 V	15.16	39.24	24.07	114.93	0.97	0.74
12 V	14.83	42.89	28.06	133.24	0.79	0.64

Table 5
Summary of the values of main parameters at the end of each heating mode test.

	T_h	T_c	ΔT	Q_h	COP_h	$COP_{h,f}$
6 V	23.21	5.25	17.96	82.78	1.91	1.01
8 V	34.96	11.32	23.63	110.56	1.52	1.00
10 V	40.07	10.93	29.14	146.14	1.31	0.98
12 V	48.48	13.30	35.17	155.50	1.02	0.82

below 1 in the two highest voltages. The decrease in the performance coefficient lowers as the input voltage increases. Consequently, at 12 V the COP drops 19%, and 25%, 34% and 47% as the voltage decreases. In heating mode, while the COP_h is above 1 in every scenario, when the consumption of the fans is included it drops and the lowest two voltage scenarios barely overcome the unit in the $COP_{h,f}$. Considering the outcomes of the COP without the auxiliary consumption, the values are in a range similar to references found in the literature [4].

5. Conclusions

This study presents the latest optimized design of the module, the aim of which was to solve the problem arising from the thermal bridge. As a result of this, a new constructive design is analyzed. The conclusions have been grouped into three sections:

- About constructive design:
  - The room has been renovated, increasing its insulation considerably. This has caused cooling problems, since in summer the heat is maintained inside and it was not possible to evacuate it properly. Although the orientation of the façade was northeast, it was necessary to improve the solar protection of the window. Therefore the need for further study regarding energy loads of the space is evident.
  - Compared to previous versions, the VATE prototype has improved sealing and insulation. Although the pre-assembly work in the laboratory has helped this, in the future it is advisable to improve the accessibility of the equipment (mainly control sensors and external fans). This is because real conditions make certain operations difficult compared to how easily they were solved under laboratory conditions.
  - The solution to transmitting the heat through the new aluminum components (see Fig. 6) has allowed an increase in insulation and a reduction in the thermal bridge, but does not eliminate it. This is an obvious factor for continuous improvement in the future.
- About design optimization:
  - Due to this increase in insulation and the new windows, the energy demand of the room is reduced. In this way, the number of TEMs installed in the prototype changes from 24 units to 16. In other words, to optimize the configuration of a VATE in the future, it is not only necessary to improve the VATE itself, but also the place in which it is located.
  - This VATE has been built with only 2 heatsinks after improving the room (compared with the previous 4), which entails an important aesthetic improvement of the prototype. This aspect is not important in terms of research, but if in the future VATEs were to be installed massively in homes or offices for example, the aesthetic improvement would be relevant for users of this technology.
  - The electrical connections, the arrangement of the Peltier cells and the monitoring equipment were optimized to achieve a more effective performance and integration. In fact, it was possible to carry out an assembly with much less wiring, which would potentially imply a cost reduction. It is therefore the first step towards the complete integration of the system in a façade, including the electric board and control system.
- About the performance:
  - Fans consume a significant amount of energy. This high fan power is an aspect to try and avoid in subsequent prototypes.
  - The higher the voltage, the higher the difference in temperature, which in turn involves a higher cooling capacity as well as a higher consumption.
  - Non-compliance with thermal transmittance. Regarding the COP values reached, although these are similar values to those found in the specialized literature (even the cooling results have improved with respect to the previous prototypes), these results still cannot compete with the current performances of any heat pump that are higher than 4, both in heating and cooling.
  - To improve this point, it would be necessary to optimize the heat transmission between the Peltier cell and the heat sinks, and to study in depth the relationship between the hot and cold sides in this kind of building application. Another point would be to carry out preliminary research in order to improve the performance of Peltier cells adapted to this range of temperatures and use.

This study represents another step forward for the integration of thermoelectric systems in building envelopes. Research suggests that a significant qualitative leap has been constructively achieved, but further development is needed to improve the selection and integration of fans, as well as their integration in other buildings during real use. It is also necessary to consider regulatory and economic aspects [12], because commercial development will not be a possibility if VATEs do not comply with these. It is worth mentioning that the Technical Building Codes do not include these active facade solutions, which could discourage the development of innovative technologies, especially for companies in the building industry.

Additionally, the value of the coefficient of thermal conductivity of the aluminum alloy can be a primary datum, because when an alloy with a high thermal conductivity is present, when the module is turned off it will logically create a greater thermal bridge

between both sides of the enclosure. However, when the module is on, the system will be more efficient, since the heat generated by the Peltier cell will be transmitted faster from the Peltier cell through the aluminum profile to the heat sink. Nonetheless, to improve the prototype would also involve studying thermoelectric research in more depth, in order to find more suitable materials for the solution that is being sought here.

The deficiencies that are observed in this type of thermoelectric technology for its implantation in conventional buildings of houses or offices should not deter us from the notion that this is a technology that may be necessary. For example, in environments such as laboratories, hospitals or spaces where security in temperature control is required, regardless of climatic conditions or the internal demand for heating and cooling. We believe that this will be a line of work for researchers in the future.

CRediT authorship contribution statement

César Martín-Gómez: Conceptualization, Methodology, Supervision, Funding acquisition. **Amaia Zuazua-Ros:** Investigation, Data curation, Visualization. **Kattalin Del Valle Lersundi:** Conceptualization, Investigation, Visualization. **Bruno Sánchez Saiz-Ezquerra:** Supervision, Writing - review & editing. **María Ibáñez-Puy:** Methodology, Investigation, Funding acquisition.

Declaration of Competing Interest

The authors declare that they have no known competing financial interests or personal relationships that could have appeared to influence the work reported in this paper.

Acknowledgement

We want to thank the support provided by the Gobierno de Navarra through the project number 0011-1365-2018-000211 "Módulo de fachada industrializado, autónomo y activo para climatización: demostración final integrada. iACTIV 2.0", co-funded by the European Regional Development Fund.

To Hydro Extruded Solutions Holding SLU Iberia, and Luis Fernando Urrea and Juan Carlos Sánchez from the Universidad de Navarra.

References

[1] D. Enescu, E.O. Virjoghe, A review on thermoelectric cooling parameters and performance, Renew. Sustain. Energy Rev. 38 (2014) 903–916, https://doi.org/10.1016/j.rser.2014.07.045.
[2] X. Han, X. Xing, H. Cheng, J. Wang, Reducing thermal conductivity of polymer derived SiC ceramics via microwave sintering processing, 2012. doi:10.4028/www.scientific.net/AMR.476-478.932
[3] C. Gayner, K.K. Kar, Recent advances in thermoelectric materials, Prog. Mater Sci. 83 (2016) 330–382, https://doi.org/10.1016/J.PMATSCI.2016.07.002.
[4] A. Zuazua-Ros, C. Martín-Gómez, E. Ibañez-Puy, M. Vidaurre-Arbizu, Y. Gelbstein, Investigation of the thermoelectric potential for heating, cooling and ventilation in buildings: Characterization options and applications, Renewable Energy 131 (2019), https://doi.org/10.1016/j.renene.2018.07.027.
[5] M. Hamid Elsheikh, D.A. Shnawah, M.F.M. Sabri, S.B.M. Said, M. Haji Hassan, M. B. Ali Bashir, M. Mohamad, A review on thermoelectric renewable energy: Principle parameters that affect their performance, Renew. Sustain. Energy Rev. 30 (2014) 337–355, https://doi.org/10.1016/J.RSER.2013.10.027.
[6] S. Riffat, G. Qiu, Comparative investigation of thermoelectric air-conditioners versus vapour compression and absorption air-conditioners, Appl. Therm. Eng. 24 (2004) 1979–1993, https://doi.org/10.1016/j.applthermaleng.2004.02.010.
[7] C. Martin-Gomez, M. Ibanez-Puy, J. Bermejo-Busto, J.A. Sacristan Fernandez, J. Carlos Ramos, A. Rivas, Thermoelectric cooling heating unit prototype, Build. Serv. Eng. Res. Technol. 37 (2016) 431–449, https://doi.org/10.1177/0143624415615533.
[8] M. Ibáñez-Puy, J.A. Sacristán-Fernández, C. Martín-Gómez, Construction of an active façade envelope with peltier cells, Int. J. Hous. Sci. Appl. 38 (2014).
[9] C. Martín-Gómez, J.C. Ramos, A. Rivas, M. Eguaras-Martínez, N. Mambrilla-Herrero, J. Torres, Prototype Thermoelectric Climate System For Its Use In Residential Buildings, in: 29th International Conference on Thermoelectrics, Shangai, China, 2010
[10] M. Ibáñez-Puy, C. Martín-Gómez, J. Bermejo-Busto, J.A. Sacristán, E. Ibañez-Puy, Ventilated Active Thermoelectric Envelope (VATE): Analysis of its energy performance when integrated in a building, Energy Build. 158 (2018) 1586–1592, https://doi.org/10.1016/j.enbuild.2017.11.037.
[11] M. Ibáñez-Puy, J. Bermejo-Busto, C. Martín-Gómez, M. Vidaurre-Arbizu, J.A. Sacristán-Fernández, Thermoelectric cooling heating unit performance under real conditions, Appl. Energy 200 (2017) 303–314, https://doi.org/10.1016/j.apenergy.2017.05.020.
[12] L. Salgado-Conrado, C. Martín-Gómez, M.I. Puy, J.A.S. Fernández, Techno-Economic Analysis of a Peltier Heating Unit System Integrated into Ventilated Façade, in: HVAC System, InTech, 2018. doi:10.5772/intechopen.76642.
[13] M. Ibáñez-Puy, J.A. Sacristán Fernández, C. Martín-Gómez, M. Vidaurre-Arbizu, Development and construction of a thermoelectric active facade module, J. Facade Des. Eng. 3 (2015) 15–25, https://doi.org/10.3233/fde-150025.
[14] A. Zuazua-Ros, C. Martín-Gómez, E. Ibáñez-Puy, M. Vidaurre-Arbizu, M. Ibáñez-Puy, Design, assembly and energy performance of a ventilated active thermoelectric envelope module for heating, Energy Build. 176 (2018) 371–379, https://doi.org/10.1016/j.enbuild.2018.07.062.
[15] E. Ibáñez-Puy, C. Martín-Gómez, J. Bermejo-Busto, A. Zuazua-Ros, Thermal and energy performance assessment of a thermoelectric heat pump integrated in an adiabatic box, Appl. Energy 228 (2018), https://doi.org/10.1016/j.apenergy.2018.06.097.
[16] C. Martín-Gómez, K. Del Valle de Lersundi, A. Zuazua-Ros, J.A. Sacristán-Fernández, M. Ibañez-Puy, Desarrollo constructivo de un prototipo de fachada termoeléctrico ubicado en la Base Antártica Gabriel de Castilla, in: VII Congreso Nacional de I+D En Defensa y Seguridad, 2019.
[17] CUI Inc., CP 60440, (n.d.).
[18] Meerstetter Engineering GmbH (2018).
[19] H.Y. Zhang, Y.C. Mui, M. Tarin, Analysis of thermoelectric cooler performance for high power electronic packages, Appl. Therm. Eng. 30 (2010) 561–568, https://doi.org/10.1016/j.applthermaleng.2009.10.020.
[20] P. Aranguren, M. Araiz, D. Astrain, Auxiliary consumption: A necessary energy that affects thermoelectric generation, Appl. Therm. Eng. 141 (2018) 990–999, https://doi.org/10.1016/J.APPLTHERMALENG.2018.06.042.